

Amplitude analysis of $B^0 \rightarrow (\pi^+ \pi^-)(K^+ \pi^-)$ decays

María Vieites Díaz,
École Polytechnique Fédérale de Lausanne

Joint Annual Meeting of the
Swiss Physical Society
and the Austrian Physical Society

26–30 August, Universität Zürich



Phenomenology of the $B^0 \rightarrow \rho^0 K^*(892)^0$ decay

Charmless B^0 meson decay reconstructed as $B^0 \rightarrow \rho^0(\pi^+\pi^-)K^*(892)^0(K^+\pi^-)$

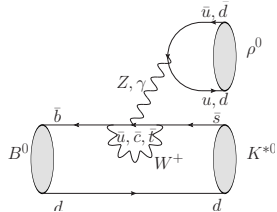
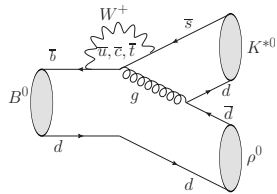
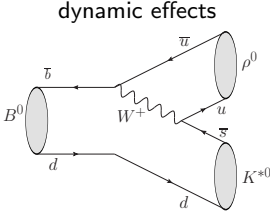
- **Proceeds via:**

- ◊ A **doubly Cabibbo suppressed tree**
- ◊ A **gluonic $b \rightarrow s$ penguin** (GP)
- ◊ A **electro-weak $b \rightarrow s$ penguin** (EWP)

→ Tree and GP diagrams have similar amplitudes → maximises interferences

- **Self-tagged** decay:
$$\begin{cases} B^0 \rightarrow (\pi^+\pi^-)(K^+\pi^-) \\ \bar{B}^0 \rightarrow (\pi^-\pi^+)(K^-\pi^+) \end{cases}$$

- **Vector resonances** → **additional CP-violating observables** and sensitivity to QCD dynamic effects

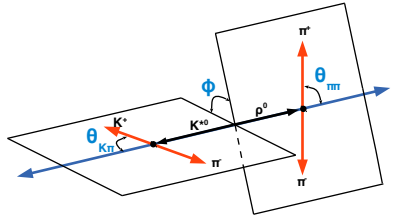


Observables in an amplitude analysis of $B \rightarrow VV$ decays

$B \rightarrow (p_a p_b)_1 (p_c p_d)_2$ decays

Can be **fully described** in terms of:

- ◇ **Three helicity angles:** θ_1, θ_2, ϕ
- ◇ **Two invariant masses:** m_1, m_2



A $B \rightarrow VV$ proceeds via **three amplitudes** \rightarrow three **spin configurations**:

P-odd $S_{VV} = 1$ and P-even $S_{VV} = 0, 2$, rotated into the transversity basis $\lambda = L, ||, \perp$.

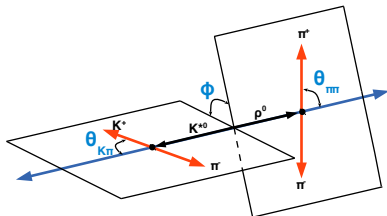
EWP diagram contributes differently to each amplitude: rich pattern of interferences.

Observables in an amplitude analysis of $B \rightarrow VV$ decays

$B \rightarrow (p_a p_b)_1 (p_c p_d)_2$ decays

Can be **fully described** in terms of:

- ◇ **Three helicity angles:** θ_1, θ_2, ϕ
- ◇ **Two invariant masses:** m_1, m_2



A $B \rightarrow VV$ proceeds via **three amplitudes** \rightarrow three **spin configurations**:

P-odd $S_{VV} = 1$ and P-even $S_{VV} = 0, 2$, rotated into the transversity basis $\lambda = L, ||, \perp$.

EWP diagram contributes differently to each amplitude: rich pattern of interferences.

Observables: number of events per amplitude (**polarisation fractions**), f^λ , and their **phase differences**:

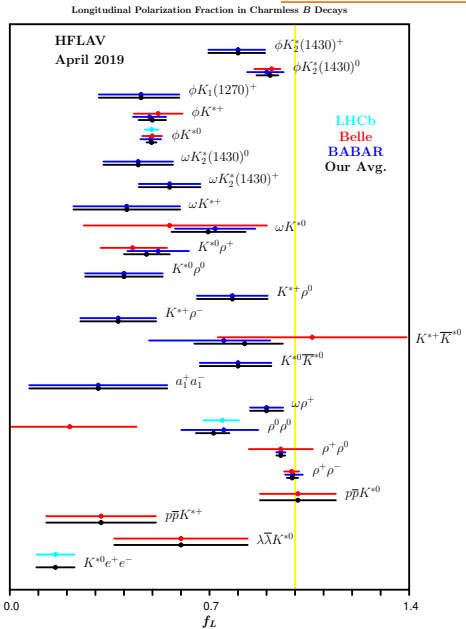
$$f^\lambda \equiv \frac{|A^\lambda|^2}{|A^L|^2 + |A^||^2 + |A^\perp|^2} \quad \delta^{\lambda_i - \lambda_j} \equiv (\delta^{\lambda_i} - \delta^{\lambda_j})$$

\rightarrow **Sensitivity to CPV by comparing B and \bar{B} parameters**

The landscape of longitudinal polarisations

Available results:

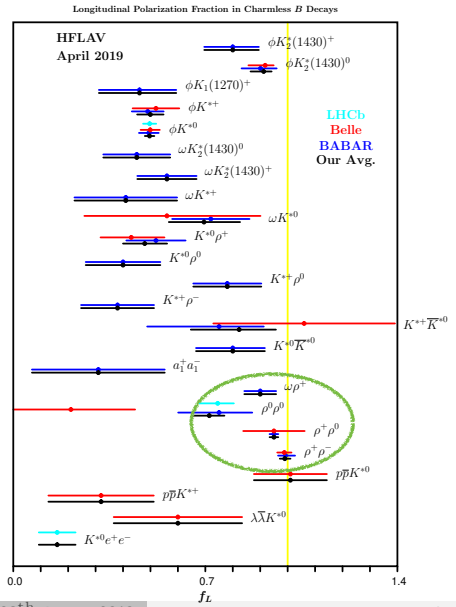
- All available measurements are CP-averaged
- Precise predictions unavailable, general dynamics not fully understood → **polarisation puzzle**
- Large f_L values confirmed in $b \rightarrow u$ tree dominated decays
- Penguin dominated modes span wider ranges



The landscape of longitudinal polarisations

Available results:

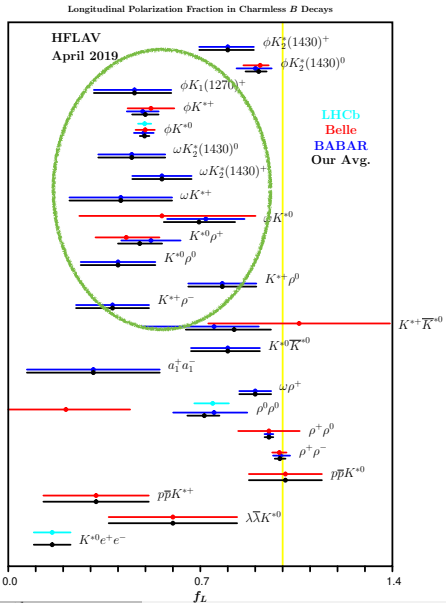
- All available measurements are CP-averaged
- Precise predictions unavailable, general dynamics not fully understood → **polarisation puzzle**
- Large f_L values confirmed in $b \rightarrow u$ tree dominated decays
- Penguin dominated modes span wider ranges



The landscape of longitudinal polarisations

Available results:

- All available measurements are CP-averaged
- Precise predictions unavailable, general dynamics not fully understood → **polarisation puzzle**
- Large f_L values confirmed in $b \rightarrow u$ tree dominated decays
- Penguin dominated modes span wider ranges

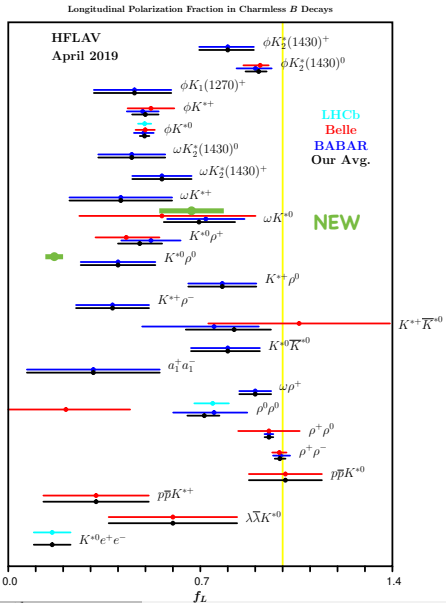


The landscape of longitudinal polarisations

Available results:

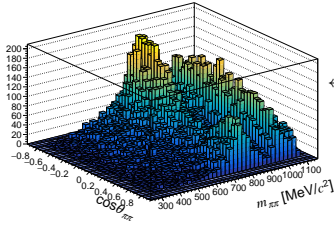
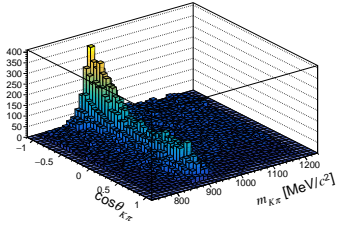
- All available measurements are CP-averaged
- Precise predictions unavailable, general dynamics not fully understood → **polarisation puzzle**
- Large f_L values confirmed in $b \rightarrow u$ tree dominated decays
- Penguin dominated modes span wider ranges

★ **Two new measurements, first observation of CPV in f_L for VV decays** (JHEP 05 (2019) 026) (LHCb Run I dataset)



Observables in an amplitude analysis of 4-body decays

In general, a \mathbf{VV} final state **cannot be uniquely selected** and other possible decay channels must be accounted for:



← Illustrative toys

Generalise to N amplitudes (isobar model):

$$d^5\Gamma \propto \Phi_4 \left| \sum_{i=1}^N A_i \cdot g_i(\cos\theta_1, \cos\theta_2, \phi) \cdot M_i(m_1, m_2) \right|^2$$

More observables: +1 amplitude, +1 phase difference per new contribution

An amplitude analysis disentangles the final state!

$A_i \rightarrow$ physical parameters

$g_i(\theta_1, \theta_2, \phi) \rightarrow$ spherical harm.

$M_i(m_1, m_2) \rightarrow$ mass prop.

Partial waves in the $B^0 \rightarrow \rho^0 K^*(892)^0$ channel

Remarks:

- ◇ Analyse a large phase-space: testing many variations of strong phase differences.

Sensitive to localised CP-violating effects!

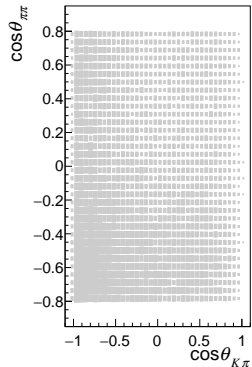
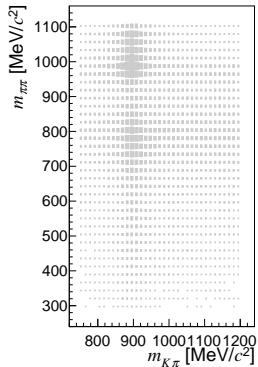
- ◇ The **invariant mass dependence** disentangles different resonances with the same spin
- ◇ The **angular dependence** separates contributions in partial waves

Partial waves:

VV: $\rho K^*, \omega K^*$, **VS:** $\rho(K\pi), \omega(K\pi)$,

SV: $[f_0(500), f_0(980), f_0(1370)]K^*$,

SS: $[f_0(500), f_0(980), f_0(1370)](K\pi)$



Partial waves in the $B^0 \rightarrow \rho^0 K^*(892)^0$ channel

Remarks:

◇ Analyse a large phase-space: testing many variations of strong phase differences.

Sensitive to localised CP-violating effects!

◇ The **invariant mass dependence** disentangles different **resonances** with the same spin

◇ The **angular dependence** separates contributions in **partial waves**

Partial waves:

VV: $\rho K^*, \omega K^*$, **VS:** $\rho(K\pi), \omega(K\pi)$,

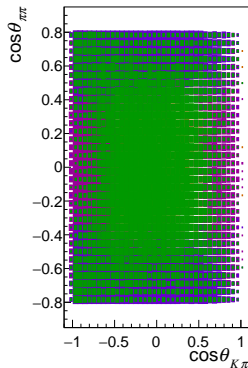
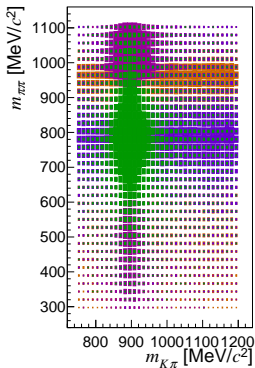
SV: $[f_0(500), f_0(980), f_0(1370)]K^*$,

SS: $[f_0(500), f_0(980), f_0(1370)](K\pi)$

*toy generated without interferences,

only contains $\sum_i |A_i|^2$

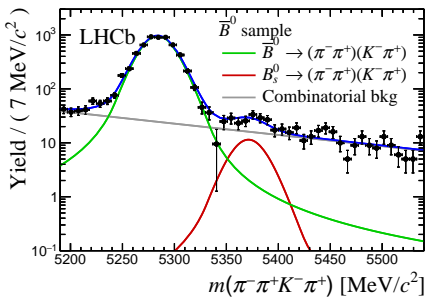
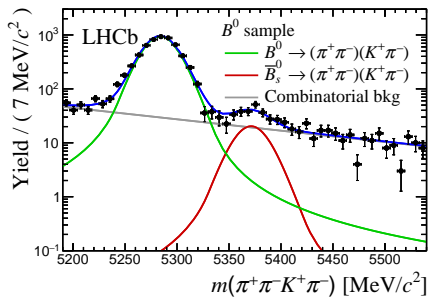
(and $(a+b)^2 \neq a^2 + b^2$)



Signal selection: four-body mass fit

→ **Used to obtain signal weights**, which allows the amplitude fit to account for the signal PDF only.

The fit is performed simultaneously in 8 categories, arising from B -meson flavour, kinematics and selection requirements (trigger).

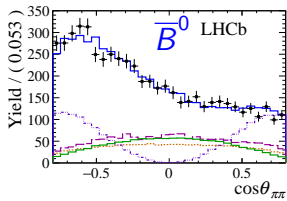
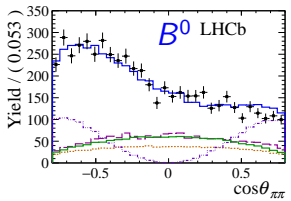


Modelling

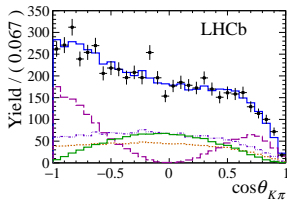
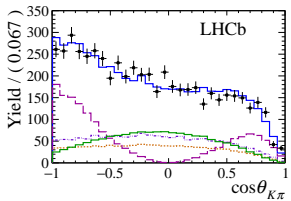
- $B_{(s)}^0$ peaks: Hypatia function
- Combinatorial: exponential function

~ 11k signal events in $B^0 + \bar{B}^0$

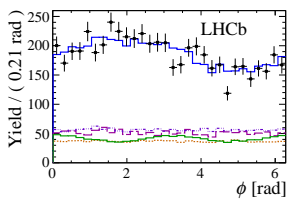
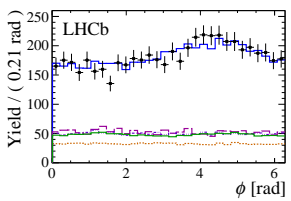
Amplitude fit (I): projections on the helicity angles



$\leftarrow \cos \theta_{\pi\pi}$



$\leftarrow \cos \theta_{K\pi}$



$\leftarrow \phi$

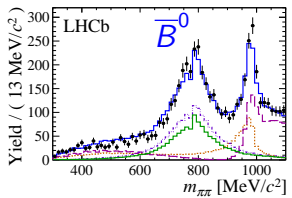
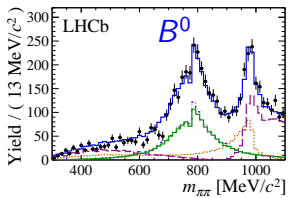
VV: $\rho K^*, \omega K^*$

VS: $\rho(K\pi), \omega(K\pi)$

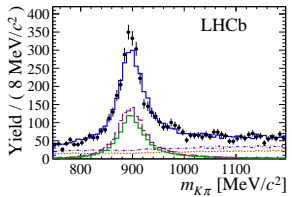
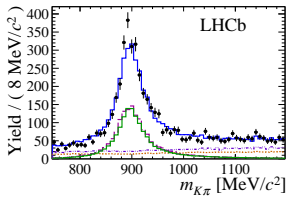
SV: $[f_0(500), f_0(980), f_0(1370)]K^*$

SS: $[f_0(500), f_0(980), f_0(1370)](K\pi)$

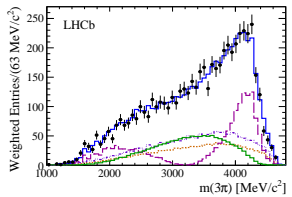
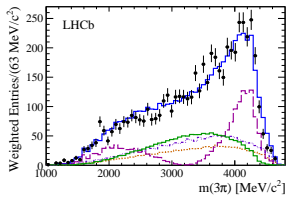
Amplitude fit(II): projections on the invariant masses



$\leftarrow m(\pi\pi)$



$\leftarrow m(K\pi)$



$\leftarrow m(\pi\pi\pi)$ (Not fitted)

VV: $\rho K^*, \omega K^*$

VS: $\rho(K\pi), \omega(K\pi)$

SV: $[f_0(500), f_0(980), f_0(1370)]K^*$

SS: $[f_0(500), f_0(980), f_0(1370)](K\pi)$

Parameter	CP average, \bar{f}	CP asymmetry, \mathcal{A}
$ A_{\rho K^*}^0 ^2$	$0.32 \pm 0.04 \pm 0.07$	$-0.75 \pm 0.07 \pm 0.17$
$ A_{\rho K^*}^{\parallel} ^2$	$0.70 \pm 0.04 \pm 0.08$	$-0.049 \pm 0.053 \pm 0.019$
$ A_{\rho K^*}^{\perp} ^2$	$0.67 \pm 0.04 \pm 0.07$	$-0.187 \pm 0.051 \pm 0.026$
$ A_{\omega K^*}^0 ^2$	$0.019 \pm 0.010 \pm 0.012$	$-0.6 \pm 0.4 \pm 0.4$
$ A_{\omega K^*}^{\parallel} ^2$	$0.0050 \pm 0.0029 \pm 0.0031$	$-0.30 \pm 0.54 \pm 0.28$
$ A_{\omega K^*}^{\perp} ^2$	$0.0020 \pm 0.0019 \pm 0.0015$	$-0.2 \pm 0.9 \pm 0.4$
$ A_{\omega(K\pi)} ^2$	$0.026 \pm 0.011 \pm 0.025$	$-0.47 \pm 0.33 \pm 0.45$
$ A_{f_0(500)K^*} ^2$	$0.53 \pm 0.05 \pm 0.10$	$-0.06 \pm 0.09 \pm 0.04$
$ A_{f_0(980)K^*} ^2$	$2.42 \pm 0.13 \pm 0.25$	$-0.022 \pm 0.052 \pm 0.023$
$ A_{f_0(1370)K^*} ^2$	$1.29 \pm 0.09 \pm 0.20$	$-0.09 \pm 0.07 \pm 0.04$
$ A_{f_0(500)(K\pi)} ^2$	$0.174 \pm 0.021 \pm 0.039$	$0.30 \pm 0.12 \pm 0.09$
$ A_{f_0(980)(K\pi)} ^2$	$1.18 \pm 0.08 \pm 0.07$	$-0.083 \pm 0.066 \pm 0.023$
$ A_{f_0(1370)(K\pi)} ^2$	$0.139 \pm 0.028 \pm 0.039$	$-0.48 \pm 0.17 \pm 0.15$
$f_{\rho K^*}^0$	$0.164 \pm 0.015 \pm 0.022$	$-0.62 \pm 0.09 \pm 0.09$
$f_{\rho K^*}^{\parallel}$	$0.435 \pm 0.016 \pm 0.042$	$0.188 \pm 0.037 \pm 0.022$
$f_{\rho K^*}^{\perp}$	$0.401 \pm 0.016 \pm 0.037$	$0.050 \pm 0.039 \pm 0.015$
$f_{\omega K^*}^0$	$0.68 \pm 0.17 \pm 0.16$	$-0.13 \pm 0.27 \pm 0.13$
$f_{\omega K^*}^{\parallel}$	$0.22 \pm 0.14 \pm 0.15$	$0.26 \pm 0.55 \pm 0.22$
$f_{\omega K^*}^{\perp}$	$0.10 \pm 0.09 \pm 0.09$	$0.3 \pm 0.8 \pm 0.4$

Parameter	CP average, $\frac{1}{2}(\delta_B + \delta_B)$ [rad]	CP difference, $\frac{1}{2}(\delta_B - \delta_B)$ [rad]
$\delta_{\rho K^*}^0$	$1.57 \pm 0.08 \pm 0.18$	$0.12 \pm 0.08 \pm 0.04$
$\delta_{\rho K^*}^{\parallel}$	$0.795 \pm 0.030 \pm 0.068$	$0.014 \pm 0.030 \pm 0.026$
$\delta_{\rho K^*}^{\perp}$	$-2.365 \pm 0.032 \pm 0.054$	$0.000 \pm 0.032 \pm 0.013$
$\delta_{\omega K^*}^0$	$-0.86 \pm 0.29 \pm 0.71$	$0.03 \pm 0.29 \pm 0.16$
$\delta_{\omega K^*}^{\parallel}$	$-1.83 \pm 0.29 \pm 0.32$	$0.59 \pm 0.29 \pm 0.07$
$\delta_{\omega K^*}^{\perp}$	$1.6 \pm 0.4 \pm 0.6$	$-0.25 \pm 0.43 \pm 0.16$
$\delta_{\omega(K\pi)}$	$-2.32 \pm 0.22 \pm 0.24$	$-0.20 \pm 0.22 \pm 0.14$
$\delta_{f_0(500)K^*}$	$-2.28 \pm 0.06 \pm 0.22$	$-0.00 \pm 0.06 \pm 0.05$
$\delta_{f_0(980)K^*}$	$0.39 \pm 0.04 \pm 0.07$	$0.018 \pm 0.038 \pm 0.022$
$\delta_{f_0(1370)K^*}$	$-2.76 \pm 0.05 \pm 0.09$	$0.076 \pm 0.051 \pm 0.025$
$\delta_{f_0(500)(K\pi)}$	$-2.80 \pm 0.09 \pm 0.21$	$-0.206 \pm 0.088 \pm 0.034$
$\delta_{f_0(980)(K\pi)}$	$-2.982 \pm 0.032 \pm 0.057$	$-0.027 \pm 0.032 \pm 0.013$
$\delta_{f_0(1370)(K\pi)}$	$1.76 \pm 0.10 \pm 0.11$	$-0.16 \pm 0.10 \pm 0.04$
$\delta_{\rho K^*}^{\parallel-\perp}$	$3.160 \pm 0.035 \pm 0.044$	$0.014 \pm 0.035 \pm 0.026$
$\delta_{\rho K^*}^{\parallel-0}$	$-0.77 \pm 0.09 \pm 0.06$	$-0.109 \pm 0.085 \pm 0.034$
$\delta_{\rho K^*}^{\perp-0}$	$-3.93 \pm 0.09 \pm 0.07$	$-0.123 \pm 0.085 \pm 0.035$
$\delta_{\omega K^*}^{\parallel-\perp}$	$-3.4 \pm 0.5 \pm 0.7$	$0.84 \pm 0.52 \pm 0.16$
$\delta_{\omega K^*}^{\parallel-0}$	$-1.0 \pm 0.4 \pm 0.6$	$0.57 \pm 0.41 \pm 0.17$
$\delta_{\omega K^*}^{\perp-0}$	$2.4 \pm 0.5 \pm 0.8$	$-0.28 \pm 0.51 \pm 0.24$

Parameter	CP average, \bar{f}	CP asymmetry, \mathcal{A}	Parameter	CP average, $\frac{1}{2}(\delta_B + \delta_B)$ [rad]	CP difference, $\frac{1}{2}(\delta_B - \delta_B)$ [rad]
$ A_{\rho K^*}^0 ^2$	$0.32 \pm 0.04 \pm 0.07$	$-0.75 \pm 0.07 \pm 0.17$	$\delta_{\rho K^*}^0$	$1.57 \pm 0.08 \pm 0.18$	$0.12 \pm 0.08 \pm 0.04$
$ A_{\rho K^*}^{\parallel} ^2$			$\delta_{\rho K^*}^{\parallel}$	$0.795 \pm 0.030 \pm 0.068$	$0.014 \pm 0.030 \pm 0.026$
$ A_{\rho K^*}^{\perp} ^2$					± 0.013
$ A_{\omega K^*}^0 ^2$					± 0.16
$ A_{\omega K^*}^{\parallel} ^2$					± 0.07
$ A_{\omega K^*}^{\perp} ^2$					± 0.16
$ A_{\omega(K)} $					± 0.14
$ A_{f_0(500)} $					± 0.05
$ A_{f_0(980)} $					± 0.022
$ A_{f_0(137)} $					± 0.025
$ A_{f_0(500)} $					± 0.034
$ A_{f_0(980)} $					± 0.013
$ A_{f_0(137)} $					± 0.04
$f_{\rho K^*}^0$					± 0.026
$f_{\rho K^*}^{\parallel}$	$0.435 \pm 0.016 \pm 0.042$	$0.188 \pm 0.037 \pm 0.022$	$\delta_{\rho K^*}^{\parallel-0}$	$-0.77 \pm 0.09 \pm 0.06$	$-0.109 \pm 0.085 \pm 0.034$
$f_{\rho K^*}^{\perp}$	$0.401 \pm 0.016 \pm 0.037$	$0.050 \pm 0.039 \pm 0.015$	$\delta_{\rho K^*}^{\perp-0}$	$-3.93 \pm 0.09 \pm 0.07$	$-0.123 \pm 0.085 \pm 0.035$
$f_{\omega K^*}^0$	$0.68 \pm 0.17 \pm 0.16$	$-0.13 \pm 0.27 \pm 0.13$	$\delta_{\omega K^*}^{\parallel-\perp}$	$-3.4 \pm 0.5 \pm 0.7$	$0.84 \pm 0.52 \pm 0.16$
$f_{\omega K^*}^{\parallel}$	$0.22 \pm 0.14 \pm 0.15$	$0.26 \pm 0.55 \pm 0.22$	$\delta_{\omega K^*}^{\parallel-0}$	$-1.0 \pm 0.4 \pm 0.6$	$0.57 \pm 0.41 \pm 0.17$
$f_{\omega K^*}^{\perp}$	$0.10 \pm 0.09 \pm 0.09$	$0.3 \pm 0.8 \pm 0.4$	$\delta_{\omega K^*}^{\perp-0}$	$2.4 \pm 0.5 \pm 0.8$	$-0.28 \pm 0.51 \pm 0.24$

Amplitudes and phase differences measured for 13 waves (CP-av. and asym.)

- ✓ First measurements for several modes
- ✓ First measurements of weak phases per channel
- ✓ First observation of CPV in angular distributions of VV decays

Detailed systematical uncertainties for the VV

- The $B^0 \rightarrow a_1(1260)^- K^+$, being sensitive to polarisations too, **dominates the systematics for the VV parameters**. S -waves are mostly affected by the parameters used in the mass propagators and the experimental resolution.

	Systematic uncertainty	$f_{\rho K^*}^0$	$f_{\rho K^*}^{\parallel}$	$f_{\rho K^*}^{\perp}$	$\delta_{\rho K^*}^{\parallel-\perp}$	$\delta_{\rho K^*}^{\parallel-0}$	$\delta_{\rho K^*}^{\perp-0}$
CP averages	Centrifugal barrier factors	0.001	0.001	0.002	0.001	–	–
	Hypatia parameters	0.001	0.001	0.001	0.001	–	–
	$B_s^0 \rightarrow K^{*0} \bar{K}^{*0}$ bkg.	0.005	0.003	0.005	0.018	0.02	0.02
	Simulation sample size	0.004	0.004	0.004	0.009	0.02	0.02
	Data-Simulation corrections	–	–	–	0.001	–	–
CP asym.	Centrifugal barrier factors	–	0.001	0.002	0.004	0.007	0.004
	Hypatia parameters	–	0.003	0.002	0.001	0.002	0.002
	$B_s^0 \rightarrow K^{*0} \bar{K}^{*0}$ bkg.	0.03	0.007	0.011	0.024	0.020	0.026
	Simulation sample size	0.02	0.010	0.009	0.011	0.027	0.023
	Data-Simulation corrections	–	0.001	0.001	–	0.002	0.002
Common (B^0, \bar{B}^0)	Mass propagators parameters	0.011	0.005	0.006	0.004	0.028	0.024
	Masses and angles resolution	0.010	0.016	0.018	0.031	0.029	0.040
	Fit method	0.003	0.001	0.002	0.003	0.005	0.004
	$a_1(1260)$ pollution	0.015	0.040	0.031	0.024	0.035	0.032
	Symmetrised ($\pi\pi$) PDF	0.004	–	0.004	0.005	0.001	0.001

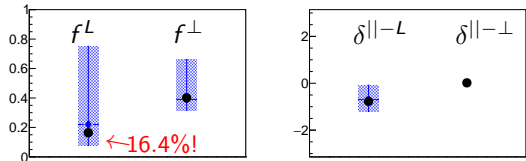
Dominant and **second dominant** systematic uncertainties.

VV numerical fit results

Remarks

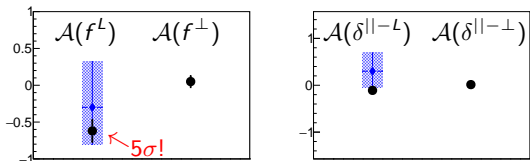
- $B^0 \rightarrow \rho^0(K^+\pi^-)$ amplitude fixed (normalisation)
- Measurements of the relative amplitudes and phases for the remaining 13 waves

CP-averages



◆ Fit results (stats. and syst. uncertainties included)

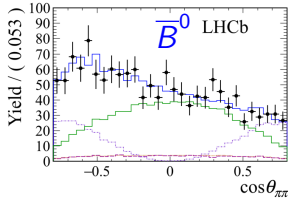
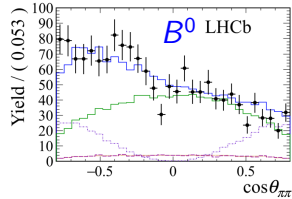
CP-asymmetries



◆ Theoretical predictions (QCDF) with uncertainties

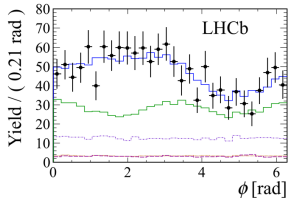
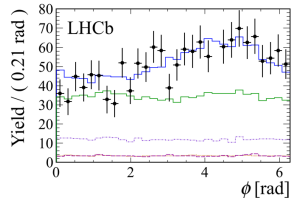
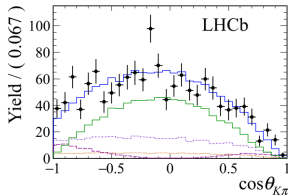
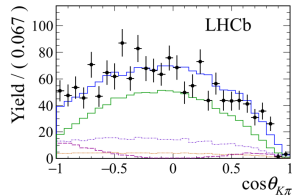
Nucl.Phys. B774 (2007) 64-101

VV dominated angular distributions



CP-violating effects can be seen in:

Different shapes of the inverted green parabola for the VV



Different oscillation in the VV

- **Amplitude analyses**

- Give access to large sets of observables probing structures of potential new contributions
- Exp.: high technicality, require careful treatment of correlations and very good understanding of the detector effects
- Th.: calculations still affected by very large uncertainties

- **Analysis of $B^0 \rightarrow (\pi^+\pi^-)(K^+\pi^-)$ decays**

- New results from the **CP averages and asymmetries** of the **polarisation fractions** together with their **phase differences**: first evidence of CPV in differential distributions of VV decays!
- Important **input to the theory community**: tests reliability of QCDF vs pQCD hypotheses (polarisation puzzle) and relevance of the EW penguin diagrams ($B \rightarrow K\pi$ puzzle)
- This work hints towards large EWP influence and is in agreement with the expectation: $f_L(\rho^0\bar{K}^{*0}) < f_L(\rho^-\bar{K}^{*0}) < f_L(\rho^0K^{*-})$

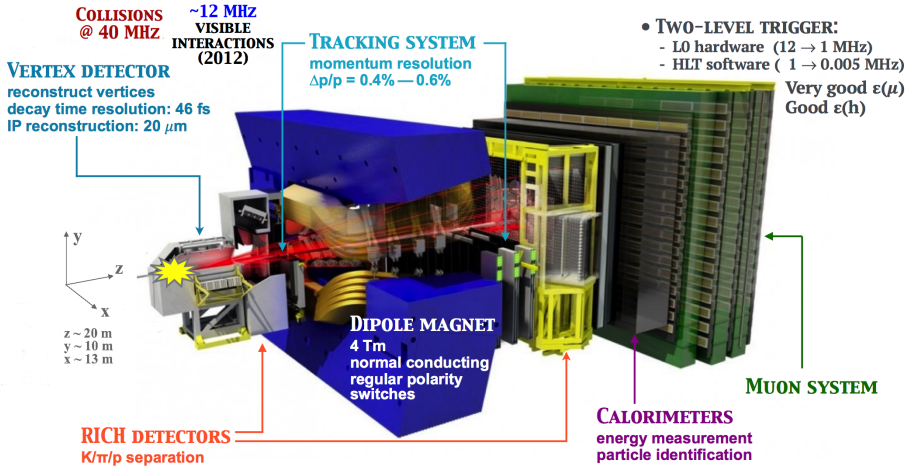
- **Amplitude analyses**
 - Give access to large sets of observables probing structures of potential new contributions
 - Exp.: high technicality, require careful treatment of correlations and very good understanding of the detector effects
 - Th.: calculations still affected by very large uncertainties
- **Analysis of $B^0 \rightarrow (\pi^+\pi^-)(K^+\pi^-)$ decays**
 - New results from the **CP averages and asymmetries** of the **polarisation fractions** together with their **phase differences**: first evidence of CPV in differential distributions of VV decays!
 - Important **input to the theory community**: tests reliability of QCDF vs pQCD hypotheses (polarisation puzzle) and relevance of the EW penguin diagrams ($B \rightarrow K\pi$ puzzle)
 - This work hints towards large EWP influence and is in agreement with the expectation: $f_L(\rho^0\bar{K}^{*0}) < f_L(\rho^-\bar{K}^{*0}) < f_L(\rho^0K^{*-})$

Thank you for your attention!
...comments, questions



Backup slides

The LHCb detector



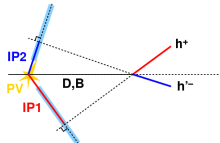
Selection summary

Event **selection** is performed in three steps:

1.- Stripping + loose preselection cuts

Geometry of B decays is preselected using soft cuts on the p_T, IP and a good track quality is required.

Soft PID cuts allow to **reconstruct** ρ^0 and $K^*(892)^0$ candidates.

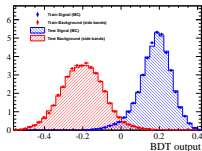


2.- Multivariate analysis + PID

A **BDT** is used to reduce the **combinatorial background**.

Charm decays are **rejected** by eliminating their phase space.

Tighter PID cuts on π^\pm and K^\pm are applied and μ^\pm are vetoed.



3.- s-Weights & Injection of simulated events

Obtain a **background subtracted** sample via **s-Weights** $\rightarrow M(K\pi\pi\pi)$ spectrum.

The **topologically similar** $B_s^0 \rightarrow K^*(892)^0 \bar{K}^*(892)^0$ decay is cancelled by **injecting simulated** $(K^+\pi^-)(K^-\pi^+)$ events.

Build a PDF describing all waves

The $B^0 \rightarrow (\pi\pi)(K\pi)$ amplitude model accounts for 10 decay channels (14 contributions):

Mass propagators

◇ ρ^0 : Gounaris-Sakurai

◇ $\omega, K^*(892)^0$:
relativistic spin-1
Breit-Wigners

◇ $f_0(500)$: spin-0
Breit-Wigner

◇ $f_0(980)$: Flatté

◇ $f_0(1370)$: spin-0
Breit-Wigner

◇ $(K\pi)_0$: LASS with a
Form Factor

i	Type	A_i	$g_i(\theta_1, \theta_2, \phi)$	$M_i(m_1, m_2)$
1		$A_{\rho K^*}^0$	$\cos\theta_1 \cos\theta_2$	$M_{\rho}(m_1)M_{K^*}(m_2)$
2	$V_1 V$	$A_{\rho K^*}^{\parallel}$	$\frac{1}{\sqrt{2}} \sin\theta_1 \sin\theta_2 \cos\phi$	$M_{\rho}(m_1)M_{K^*}(m_2)$
3		$A_{\rho K^*}^{\perp}$	$\frac{i}{\sqrt{2}} \sin\theta_1 \sin\theta_2 \sin\phi$	$M_{\rho}(m_1)M_{K^*}(m_2)$
4		$A_{\omega K^*}^0$	$\cos\theta_1 \cos\theta_2$	$M_{\omega}(m_1)M_{K^*}(m_2)$
5	$V_2 V$	$A_{\omega K^*}^{\parallel}$	$\frac{1}{\sqrt{2}} \sin\theta_1 \sin\theta_2 \cos\phi$	$M_{\omega}(m_1)M_{K^*}(m_2)$
6		$A_{\omega K^*}^{\perp}$	$\frac{i}{\sqrt{2}} \sin\theta_1 \sin\theta_2 \sin\phi$	$M_{\omega}(m_1)M_{K^*}(m_2)$
7	$V_1 S$	$A_{\rho(K\pi)}^0$	$\frac{1}{\sqrt{3}} \cos\theta_1$	$M_{\rho}(m_1)M_{(K\pi)}(m_2)$
8	$V_2 S$	$A_{\omega(K\pi)}^0$	$\frac{1}{\sqrt{3}} \cos\theta_1$	$M_{\omega}(m_1)M_{(K\pi)}(m_2)$
9	$S_1 V$	$A_{f_0(500)K^*}^0$	$\frac{1}{\sqrt{3}} \cos\theta_2$	$M_{f_0(500)}(m_1)M_{K^*}(m_2)$
10	$S_2 V$	$A_{f_0(980)K^*}^0$	$\frac{1}{\sqrt{3}} \cos\theta_2$	$M_{f_0(980)}(m_1)M_{K^*}(m_2)$
11	$S_3 V$	$A_{f_0(1370)K^*}^0$	$\frac{1}{\sqrt{3}} \cos\theta_2$	$M_{f_0(1370)}(m_1)M_{K^*}(m_2)$
12	$S_1 S$	$A_{f_0(500)(K\pi)}^0$	$\frac{1}{3}$	$M_{f_0(500)}(m_1)M_{(K\pi)}(m_2)$
13	$S_2 S$	$A_{f_0(980)(K\pi)}^0$	$\frac{1}{3}$	$M_{f_0(980)}(m_1)M_{(K\pi)}(m_2)$
14	$S_3 S$	$A_{f_0(1370)(K\pi)}^0$	$\frac{1}{3}$	$M_{f_0(1370)}(m_1)M_{(K\pi)}(m_2)$

Account for the \bar{B} decay: $A_i \rightarrow \eta_i \bar{A}_i$; with η_i the parity of each amplitude:

$$\eta_{A_i} = 1 \text{ except for } \eta_{A_{\perp}} = -1$$

Sources of systematic uncertainties

$$\text{PDF term} \sim \frac{\mathcal{A}_i \cdot g_i(\theta_1, \theta_2, \phi) \cdot \mathcal{M}_i(m_1, m_2) \times (\dots)_j^*}{\sum_{i,j} \mathcal{A}_i \mathcal{A}_j^* n_{w_{ij}}}$$

Normalisation: $\sum_{i,j} \mathcal{A}_i \mathcal{A}_j^* n_{w_{ij}}$

- $\mathcal{A}_i \mathcal{A}_j^* \rightarrow$ polarisation affects acceptance.
- $n_{w_{ij}}$ obtained from MC sample, limited statistics
- $n_{w_{ij}}$: data-simulation corrections (PID, p_T^B and Ntracks)

Mass propagators: $\mathcal{M}(m_1, m_2)$

- Vary the parameters in the propagators: $BW(m, L, m_0, \Gamma_0, r_0) \rightarrow x_0 \rightarrow \text{Gauss}(x_0, \sigma_{x_0})$

Pull distributions: to estimate possible model-induced biases

Neglected contributions in the model:

- $\mathcal{A}_i \mathcal{A}_j^*$: identical π exchange, $B^0 \rightarrow (\pi^+ \pi^-)(K^+ \pi^-)$, and $B^0 \rightarrow a_1(1240)^- K^+$ pollution
- $\theta_1, \theta_2, \phi, m_1, m_2$: experimental resolution and orbital angular momentum barriers

Data sample:

- Negative weights cancelling the $B_s^0 \rightarrow K^*(892)^0 \bar{K}^*(892)^0$ contribution (yield and shapes)
- Signal weights from the sFit

Fitting frameworks

The $B^0 \rightarrow (\pi\pi)(K\pi)$ PDF model was implemented in three different frameworks:

● Minit + CPU: RooFit based

- Fully implemented in ROOT, was the first option for historical reasons
- **Slow**: fits toy-MC in 15min
- Has trouble converging with many (>20) free parameters in several dimensions with weighted data (spoil $\log \mathcal{L}$ smoothness)
- ✓ **toy-MC generation**

● Minit + GPU: Ipanema based

→Ipanema@arXiv

- Same methods as above, but implemented in Python + pyCUDA
- **Very fast**: fits toy-MC in 18s
- Still relies on Minit → same issues with weighted data as above
- ✓ **toy-MC based systematics (fits)**

● MultiNest + GPU: Ipanema based

→Multinest project

- Implemented in Python + pyMultinest + pyCUDA
- Uses nested sampling → performs good with weighted samples
- Scans the whole parameter space → **very slow** (fits toy MC in 3h)
- ✓ **nominal fit + data based systematics**

A glimpse into MultiNest

Uses **clustered nested sampling**: a **Monte Carlo** method targetted at the efficient calculation of the probability for a set of parameter values given a data sample

Mon. Not. R. Astron. Soc. **000**, 1–14 (2008) Printed 19 September 2008 (MN 19jx style file v2.2)

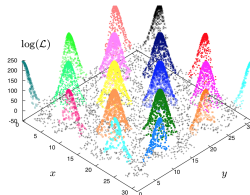
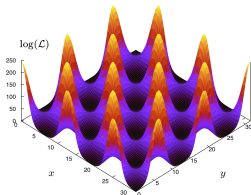
MULTINEST: an efficient and robust Bayesian inference tool for cosmology and particle physics

F. Feroz*, M.P. Hobson and M. Bridges
Astrophysics Group, Cavendish Laboratory, JJ Thomson Avenue, Cambridge CB3 0HE, UK

Highlighted characteristics:

- Defines “high dimensionality” as $> 50D$:-)
- **Nested sampling**: new algorithm type (~ 2004) performing better (less evaluations needed) than MC-Markov-Chain reference
- **Clustered** nested sampling: very good finding several modes in the posterior distributions (induced by non smoothness of the $\log \mathcal{L}$ in our case)
- Very slow **but**: parameter estimation, uncertainties, $\log \mathcal{L}$ profiles, iso- $\log \mathcal{L}$ contours, correlations, ... **all produced at once**

Example of MultiNest performance finding peaks in a multimodal $\log \mathcal{L}$ distribution. Toy (left) vs fit (right).



Goal: perform a maximum likelihood fit of the PDF model \rightarrow compute the sum

$$\frac{1}{N} \sum_e^N \log \left(\frac{|\text{PDF}_e|^2}{\int_{\mathcal{D}} |\text{PDF}|^2} \right)$$

- PDF_e is the PDF evaluated for event e and N , the total number of events
- \mathcal{D} : 5D integration domain \rightarrow shaped by the LHCb detector acceptance and the selection requirements \Rightarrow not easy to parametrise as $f(\theta_1, \theta_2, \phi, m_1, m_2)$.

Relevance of \mathcal{D} :

- Defines the **normalisation of the PDF**
- Lack of analytical expression for \mathcal{D} : the 5D integral has to be done **numerically**.

In general, it will be needed to:

- \rightarrow Rely on simulated samples (MC) to characterise \mathcal{D}
- \rightarrow Analyse different domains separately
- \rightarrow Use an approximation to obtain an analytical expression allowing to generate toys
- \rightarrow Control the normalisation of the PDF in the fit